International Journal of Modern Physics C, Vol. 11, No. 8 (2000) 1567–1580
© World Scientific Publishing Company

MELTING AND FRAGMENTATION OF NICKEL NANOPARTICLES: MOLECULAR–DYNAMICS SIMULATIONS

BILAL GÜNEŞ

Department of Physics, Gazi Education Faculty, Gazi University
06500 Ankara, Turkey

ŞAKIR ERKOÇ*

Department of Physics, Middle East Technical University
06531 Ankara, Turkey
E-mail: erkoc@erkoc.physics.metu.edu.tr

Received 12 January 2001
Revised 16 January 2001

Melting and fragmentation behaviors of Ni_{429} cluster have been studied with molecular-dynamics simulations using a size-dependent empirical model potential energy function. To monitor thermal behaviors of the cluster, we calculated some physical quantities such as average potential energy per atom, specific heat, radial atomic distribution, bond length distribution, average interatomic distance, nearest neighbor distance and average coordination number as a function of temperature. The roles of the surface and core atoms in the melting and fragmentation process of the cluster are also investigated by considering the surface and the bulk coordination numbers of the cluster.

Keywords: Nickel Clusters; Melting; Fragmentation; Empirical Potentials; Nanoparticles; Molecular-Dynamics.

PACS Nos: 36.40.–c, 36.40.Qv, 61.46.+w, 02.70.Ns.

1. Introduction

Clusters play an important role to understand the transition from the microscopic structure to the macroscopic structure of matter. Nickel clusters are interesting and have potential importance in the physics and chemistry of transition metals.[5] Nickel clusters are of special interest because of their practical applications in ferromagnetism and their superparamagnetic behavior.[6,7]

The phase transition of the clusters have been intensively studied both theoretically and experimentally.[8–23] Early theories of melting have focused on the role of the instabilities of the solid.[24] More recent theories have been emphasized the role of defects and external surfaces.[25,26] From molecular-dynamics studies, there is

*Corresponding author.

considerable evidence that melting is initiated at external surfaces or along internal defects such as grain boundaries or dislocations. The further study of melting in the small clusters is relevant to a better understanding of the melting transition for the effect of the size of the cluster: as cluster size decreases, the fraction of the surface atoms increases and any role played by the surface in the melting transition will be given more importance.[27] All these studies show that (a) the melting temperature of the clusters is lower than the melting temperature of a perfect finite solid and (b) the surface melting temperature is expected to be lower than the overall melting temperature because of disorder appearing first at the surface of the cluster as a result of the fact that the average coordination number of the surface atoms is less than that of the bulk atoms for a cluster of certain size.[28]

In this study, we monitored some physical quantities to determine the phase transition of the cluster and considered average, surface, and bulk coordination number separately to compare the surface and the overall melting and fragmentation temperatures of the cluster.

2. The Potential Energy Function and the Method of Calculations

In this work, we have used a size dependent empirical potential energy function (SDEPEF) developed for a finite system and parameterized and applied for nickel.[1,2] The total interaction energy (Φ) of an N particle system may be calculated from the sum of pair interactions and scaled by a size dependent function $f(N)$,

$$\Phi = f(N) \sum_{i<j}^{N} U(r_{ij}) \,. \tag{1}$$

The pair potential energy function $U(r)$ has the form,[3,4]

$$U(r) = A \left[\left(\frac{r_0}{r} \right)^{2n} e^{-2\alpha(r/r_0)^2} - \left(\frac{r_0}{r} \right)^{n} e^{-\alpha(r/r_0)^2} \right] . \tag{2}$$

The size dependent function $f(N)$ has the form,[1]

$$f(N) = \sqrt{\beta_1 + \beta_2 / N} \,. \tag{3}$$

The potential parameters used for nickel are: $A = 8.28$, $r_0 = 2.2$, $n = 2.89247$, $\alpha = 0.693147181$,[3,4] and $\beta_1 = 0.081$, $\beta_2 = 1.532$.[1] In these parameters, energy is in eV and distance is in Å.

Molecular-dynamics simulations were performed using the Nordsieck–Gear algorithm[29,30] within the seventh order predictor-corrector method[31] with a time step 1.0×10^{-15} s. We performed simulations at temperatures from 50 to 5100 K with steps of 50 K, the initial configuration is relaxed at 1 K. At each temperature raise, the system is relaxed for 50 000 MD steps to get the average of the physical quantities used to investigate thermal behaviors of the cluster.

In order to characterize the thermal behavior of the cluster as a function of increasing temperature, we monitored the following quantities,

(a) The caloric curve which is a plot of the average potential energy per atom versus temperature.

(b) The reduced specific heat defined as:

$$C/Nk_B = \frac{\langle E^2\rangle - \langle E\rangle^2}{N(k_BT)^2}\,, \tag{4}$$

where $\langle\,\rangle$ denotes average over the entire trajectory, N is the number of the atoms in the cluster, E is the average potential energy per atom and k_B is the Boltzmann constant.

(c) The average interatomic distance given by:

$$d_{\text{av}} = \frac{2}{N(N-1)}\sum_{i<j}^{N} r_{ij}\,, \tag{5}$$

where r_{ij} is the distance between atoms i and j.

(d) The nearest-neighbor distance d_{nn}.

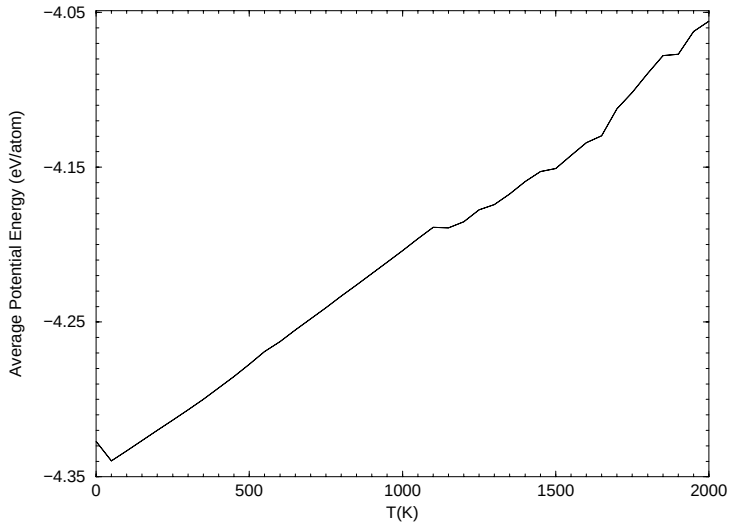
(e) The average coordination number defined as:

$$C_{\text{av}} = \frac{1}{N}\sum_{i=1}^{N} c_i\,, \tag{6}$$

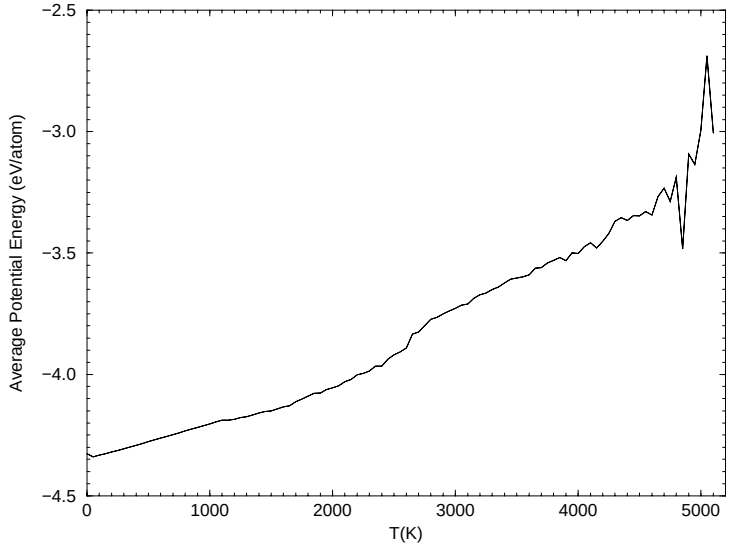
where c_i is the coordination number of atom i. In addition to these physical quantities, the radial atomic distribution and bond length distribution for some critic temperatures are also calculated to check whether the cluster exhibits solid-like or liquid-like behavior at a particular temperature.

3. Results and Discussion

Figure 1 shows the variation of the average potential energy of the cluster as a function of temperature (caloric curve). The average potential energy increases monotonically with temperature in the range $T \leq 1150$ K, but, it begins to jump at a temperature $T_s = 1150$ K. T_s can be defined as the surface melting temperature of the cluster.[28] The abrupt change in the average potential energy indicates that the cluster undergoes a phase change. The average potential energy rises up from 1150 K to 1650 K, this temperature range is the phase transition region in which the cluster transforms from a near-rigid, solid-like, structure to a nonrigid, liquid-like, structure but remains bound for thousands of vibrational periods. The absence of the sharp change in the slope of the energy, unlike in the bulk, is an indication of a finite-size effect, and appears because the clusters are able to contain both of the phases at the same temperature.[27] We took the midpoint of this significantly rising region in the energy with the temperature, $T_m = 1400$ K, as the overall melting temperature of the cluster at which melting takes place. These critic temperature values are also checked using other physical quantities discussed below.



(a)



(b)

Fig. 1. Caloric curve of the cluster: the average potential energy per atom versus temperature in the range (a) $1 \leq T \leq 2000$ K, (b) $1 \leq T \leq 5100$ K.

Figure 2 shows the specific heat in units Nk_B for the cluster as a function of temperature. A common feature in this figure is the presence of more than one peak in the specific heat. It can be said that cluster melts in two stages at $\approx$ 500 K and $\approx$ 1400 K. The peak at $\approx$ 500 K can be explained by considering

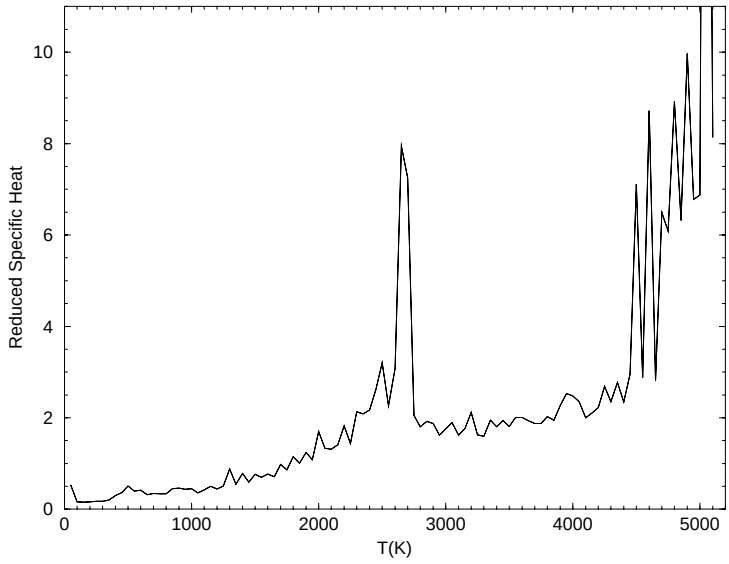


Fig. 2. Specific heat divided by Nk_B, C/Nk_B, versus temperature. The height of the last peak at about 5000 K reaches upto 33.

the terms of premelting phenomenon, surface melting and surface reconstruction. Premelting followed by bulk melting was reported[32,33] to be characteristic of open-shell nickel clusters (i.e., clusters with geometries where the outer shells are not fully decorated with atoms) such as Ni_n, $14 \leq n \leq 18$. The premelting behavior is strongly influenced by vacancies and anharmonicities which are distinctly larger in open shell clusters than in closed-shell clusters. The surface atoms which do not belong to the complete shell are, in generally, more weakly bound than the atoms in the cluster, and, therefore, the amplitudes of these atoms are significantly larger than those in closed-shell clusters. This gives rise to enhanced harmonicities and provides fluidity in the system at lower temperature, a fact that leads to premelting behavior in these clusters. The clusters of Ni_{14}, Ni_{15}, Ni_{16}, Ni_{17} and Ni_{20} were reported to show premelting phenomenon while the clusters of Ni_{13} and Ni_{19} show no premelting phenomenon.[27,34] The difference in these cluster groups is whether or not the cluster has one or more extra atom(s) outside stable icosahedral core atoms. Ni_{13} and Ni_{19} clusters have the complete atomic shell geometries, namely one and double highly stable icosahedral core atoms respectively, and they do not show premelting phenomenon. On the other hand, Ni_{14}, Ni_{15}, Ni_{16} and Ni_{17} clusters have respectively, one, two, three and four extra atoms outside the Ni_{13} core and Ni_{20} cluster has one atom outside a very stable double icosahedral Ni_{19} core.

The premelting is similar to the surface melting phenomenon observed in the bulk crystals and arises because of the difference in coordination numbers between the atoms on the surface and the atoms in the bulk. When we consider our cluster at this point, Ni_{429} cluster has also the complete atomic shell geometries and does

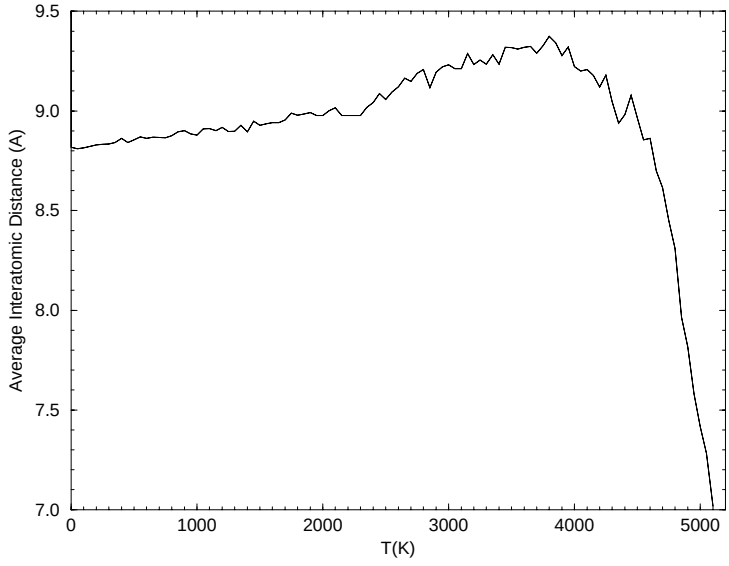


Fig. 3. Average interatomic distance d_{av} versus temperature.

not have any more atom outside the core, like Ni_{13} and Ni_{19} clusters, while it shows premelting-like phenomenon, unlike Ni_{13} and Ni_{19} clusters. This discrepancy can be attributed to the cluster size effect. In the small sizes, surface to core atoms ratio is higher and phase transition is easily controlled by surface atoms whereas in the larger sizes, the role played by surface atoms is becoming less important.[35,36] In the larger clusters, premelting is appearing due to surface reconstruction even though the cluster has the complete atomic shell and no extra atoms outside the core.

The plot of the average interatomic distance d_{av} as a function of temperature (see Fig. 3) is another indicator of thermal transition of the cluster, d_{av} is expected to increase with the increasing temperature and the abrupt increase in d_{av} is a signal of structural changes in the cluster.[37,38] It is reported[38] that at $d_{\mathrm{av}} = 1.05$ (d_{av} is normalized to its value at the beginning of the transient), the onset fragmentation took place for clusters of all compositions studied. Premelting behavior and melting of the clusters are clearly deduced from the irregular shape at these temperature regions as seen in Fig. 3.

The variation of nearest-neighbor distance d_{nn} and average coordination number with the temperature is also calculated and plotted in Figs. 4 and 5 respectively. As the temperature increases, the variation of d_{nn} is expected to increase regularly, any abrupt change of this variation can be considered as an indicator of the structural phase transition. The irregular changes take place at about 500 and 1400 K in Fig. 4. The function of the mean coordination number to the melting and fragmentation process is discussed below.

Bond-length distribution as a function of interatomic distance is shown in Fig. 6. The mean value of the distance between the pairs of atoms which are nearest

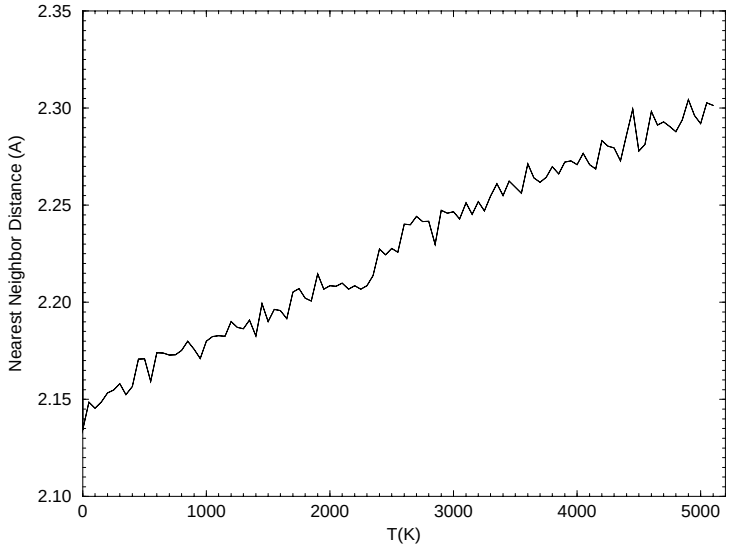


Fig. 4. Nearest neighbor distance d_{nn} versus temperature.

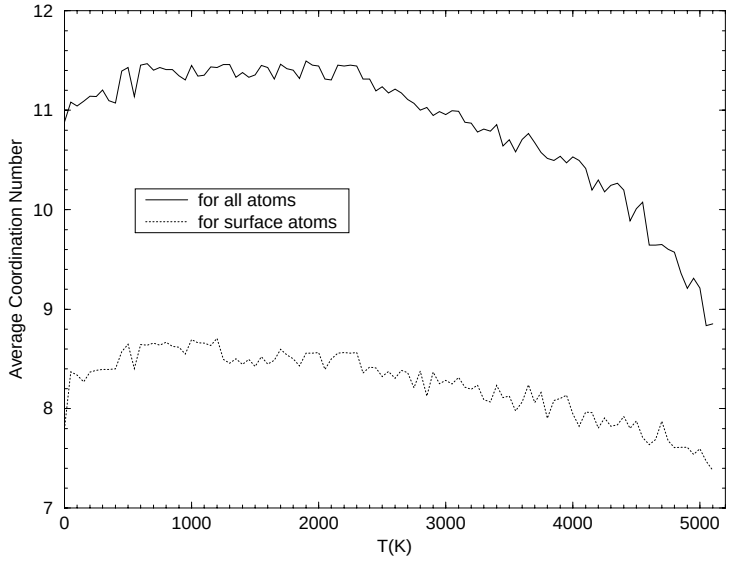


Fig. 5. Average coordination number $C_{\rm av}$ versus temperature.

neighbors in the initial configuration is calculated and monitored as increasing temperature. Bond-length distribution is used to determine structural properties of the cluster and based on the following physical fact.[39] In a solid rigid state, the atoms always execute small-amplitude oscillations around equilibrium positions which are distributed in such a way that the nearest atoms of any atom of the cluster

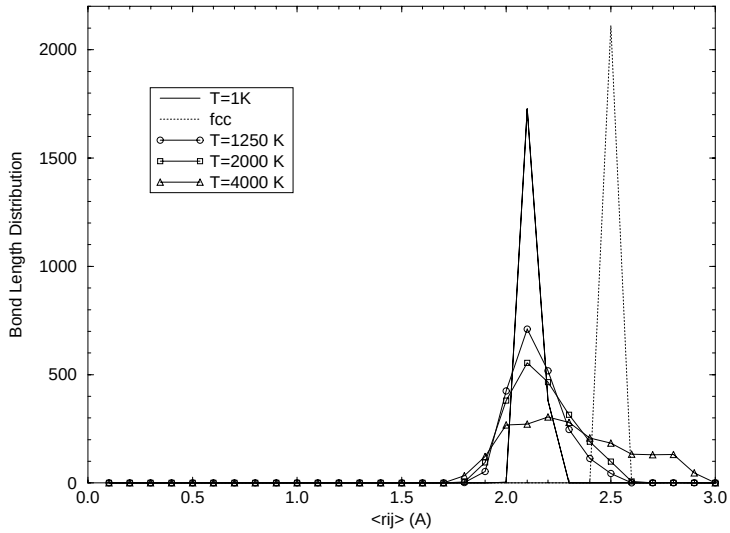
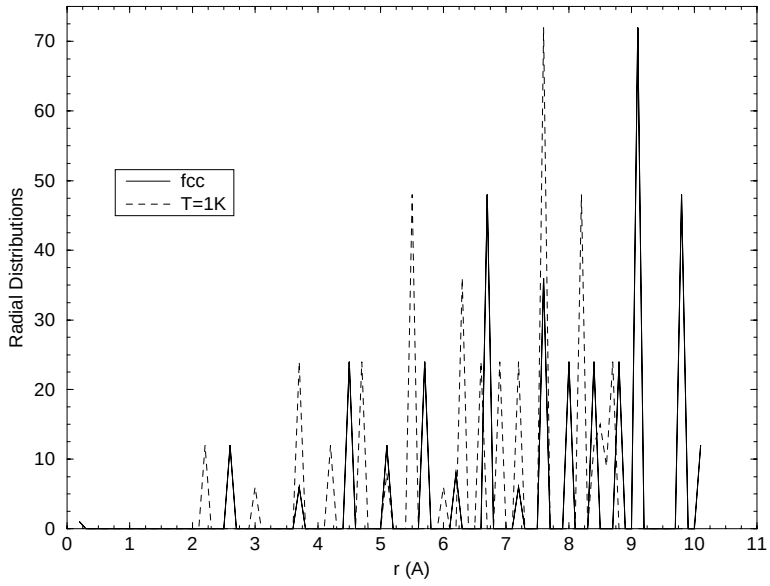


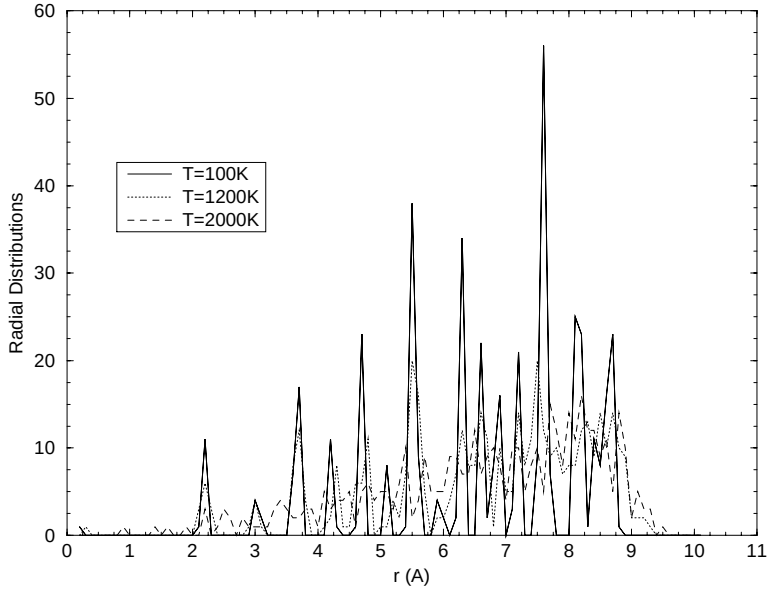
Fig. 6. Bond-length distribution (distribution of the mean value of the distance between the pairs of atoms which are initially nearest neighbors in the solid state) versus interatomic distance at various temperatures.

can be easily defined and determined. However, in the liquid state, the nearest atoms of a given atom can no longer be defined and determined as in a solid state. In a liquid state, there is a bond-exchange process between the atoms so that any two atoms of the cluster can lie at either the nearest or the farthest distance. As shown in Fig. 6, there is only a single peak around bond length between nearest-neighbor atoms at low temperatures which indicates that the cluster is in the solid state. Upon increasing the temperature because of the occurrence of the bond-exchange process between the atoms, the width of single peak at the beginning starts to increase and then a second peak appears in the distributions of the interatomic distance. Increasing of the peak width, decreasing of the peak height and appearing of a second peak are indicators of the structural transformation from solid-like cluster to liquid-like one.

Figure 7 shows radial distribution function as a function of the cluster radius which is one of the geometric quantity, such as average interatomic distance, bond-length distribution and average coordination number that reflects the information about the structure of the cluster as used previously.[37,40] For radial atomic distribution, two limiting cases are of interest: in a pure crystal, it consists of a series of peaks, located at the various interatomic separations. It is zero between the peaks. At the other extreme, if atomic centers are randomly distributed throughout the material, then, the average concentration does not depend on radius. The liquid, an intermediate phase of the two extremes pointed out above, displays short-range order but not long-order while the crystal shows both short and long-range order. When a cluster is generated from the crystalline structure, the atomic positions



(a)



(b)

Fig. 7. Radial atomic distributions expressed as numbers of atoms N versus distance from the center of mass of the cluster r, (a) for f.c.c. crystal and at $T = 1$ K, (b) at $T = 100$ K, 1200 K and 2000 K.

cannot be kept at their original places particularly the atoms at and near the surface region displace even at low temperature. Figure 7(a) shows this situation clearly. Figure 7 shows that at low temperature, the cluster consists first and second-nearest-neighbor peaks and the satellite peaks coincide exactly with those in the crystal described above. On the other hand, at high temperature, the peaks are becoming shapeless at large radius while the peaks are remaining the form at short radius. These features are typical of the liquid phase.[41]

According to the recent studies, it is possible to predict the melting temperature of the cluster using average coordination number in the cluster. The criterion to predict the melting temperature is suggested as[42]:

$$T_m = \frac{C_m}{C_b} T_b \,, \tag{7}$$

where T_m and T_b are the overall melting temperatures of the cluster and the bulk material respectively, C_m and C_b are the mean coordination number of the atoms in the cluster and the bulk respectively ($C_b = 12$ for f.c.c. metals, $T_b = 1728$ K for Ni[43]). To predict the surface melting temperature of the cluster, Eq. (7) is reformulated as the following,[28]

$$T_s = \frac{C_s}{C_b} T_b \,, \tag{8}$$

where T_s is the surface melting temperature of the cluster and C_s is the mean surface atomic coordination number in the cluster. Equation (7) leads to a size dependence as[44,45]:

$$T_m = T_b - AN^{-1/3} \,, \tag{9}$$

where A is a positive constant which depends on temperature and pressure and N is the number of atoms in the cluster. This equation expresses the fact that the melting temperature of the cluster is low when cluster is small and approaches the bulk melting temperature as the number of atoms of the cluster increases. To compare the roles of the surface atoms and core atoms of the cluster to the melting process, we calculated average, surface and bulk coordination numbers, separately, and used the above equations, Eqs. (7)–(9). The results of the present study are compared with literature values in Table 1. From these results: (a) the overall melting temperature of the cluster is lower than that of the bulk material, (b) the surface melting temperature is lower than the overall melting temperature for the cluster, (c) the melting of the cluster depends on the cluster size. The lower surface melting temperature compared to the overall one for a cluster is attributed to the fact that the core atoms of the cluster have a higher coordination number than the surface atoms. As the cluster heats up, disorder first appears at the surface resulting in the surface melting. The size effect studies suggest[35,36,46,47] that as the cluster size decreases, the fraction of the surface atoms increases and phase transition is dictated by the surface atoms. As the cluster size increases, the number

Table 1. The surface and overall melting temperatures namely T_s and T_m respectively for the Ni clusters. T_m^* and T_s^* are calculated from Eqs. (7) and (8) respectively, the constant A is from Eq. (9) (this value is not originally calculated in Ref. 28). The bulk temperature $T_b = 1728$ K and the bulk coordination number $C_b = 12$ for Ni crystal.[43]

Cluster	C_m	C_s	T_m	T_s	T_m^*	T_s^*	A	Ref.
Ni_{429}	9.85	7.95	1400	1150	1418	1144	2338	This work
Ni_{55}	8.51	7.43	1225	1050	1224	1069	1916	28
Ni_{13}	6.46	6.00	950	850	929	863	1878	28

of the surface atoms decreases and melting temperature of the cluster regularly increases up to the melting temperature of the bulk limit as shown in Table 1.

We extended the simulation to the cluster fragmentation. In the literature, as the indicator of the structural changes in fragmentation, caloric curve, average interatomic distance and radial distribution function are used.[37,38,48,49] Alternatively, the activation and the other forms of energy relations are used to directly calculate the number of the atoms evaporating from the surface.[44,45,50,51] An abrupt increase of average interatomic distance d_{av} is considering as a signal of fragmentation, so, we monitor the fragmentation process by using d_{av}. It is reported that the onset of fragmentation takes place at $d_{\text{av}} \approx 1.05$ where d_{av} is normalized by its value at the beginning.[38] In the present study, a single atom is separated from the system (first separation) at $T_e = 2750$ K, the second separation takes place at $T = 3100$ K, at these temperatures, d_{av} is 1.042 and 1.045 respectively as shown in Fig. 3. These separations may be considered as the evaporation of the system. The number of the evaporating atoms begins to increase above $T = 3850$ K where $d_{\text{av}} = 1.060$ which indicates that the cluster undergoes fast structural changes. For comparison, in bulk Ni, the boiling point is $T = 3005$ K,[52] our results indicate that the evaporation of the cluster is observed at a lower temperature than in the bulk, as observed for melting temperature discussed above. It is reported for Ag_6 cluster that the melting temperature in the cluster is lower than in the bulk, but, evaporation is observed almost at the same temperature.[53]

In the liquid state, the coordination number of the atoms has no longer meaningful as it has in the solid state, but, the cluster in the liquid state still remains short-range order and bound for thousands of vibrational periods. In the light of these physical facts, to check the validity of Eq. (7) for fragmentation process, we modified Eq. (7) as replacing T_m, T_b and C_m by T_e, T_{boil} and C_e respectively as the following,

$$T_e = \frac{C_e}{C_b} T_{\text{boil}} , \tag{10}$$

where T_e is the temperature at which the first atom evaporates, T_{boil} is the boiling point of the bulk materials (3005 K[52]), C_e is the mean coordination number of atoms in the liquid phase of the cluster (in the range of 2500 K $\leq T \leq$ 3500 K, around

the fragmentation taking place, C_e is calculated as 10.96), and C_b is the mean coordination number of the atoms in the bulk (12 for f.c.c. metals). This equation gives $T_e = 2745$ K which is fairly in agreement with observed value 2750 K. By inserting these values to the modified form of the Eq. (9), namely $T_e = T_{\text{boil}} - AN^{-1/3}$, the positive constant is calculated as $A = 1923$. If one uses the values of Eq. (8) in Eq. (9), constant A then takes the value of 2338.

4. Conclusions

We have investigated melting and fragmentation behaviors of Ni_{429} cluster with molecular-dynamics simulations using a size-dependent empirical model potential energy function. Phase transition of the cluster is probed using some physical quantities. It has been found that, with increasing temperature, the cluster undergoes, firstly, solid-to-solid transition at about 500 K, then, solid-like to liquid-like transition at about 1400 K. Lastly, atoms begin to vaporize from the cluster at 2750 K. We may state the results of this work as the following: (a) the overall melting temperature of the cluster is lower than that of the bulk materials due to the fact that the mean coordination number of the atoms in the cluster is less than that of the bulk atoms, $T_m < T_b$, (b) the surface melting temperature of the cluster is lower than the overall melting temperature of the cluster for a certain size due to the fact that the mean coordination number of the surface atom is less than that of the core atom, $T_s < T_m$, (c) the fragmentation takes place at the lower temperature than the boiling point of the bulk material because of the lower coordination number of the atoms in the cluster, $T_e < T_{\text{boil}}$, and finally (e) two stages melting process takes place, which is clearly seen in the specific heat curve and in the other indicator discussed above, as a result of premelting phenomena which occurs in very different ways depending on the size. In the small sizes, the clusters which have only closed shells and do not have any more atom outside the core, do not show premelting phenomena whereas the clusters which have one or more atom(s) outside the core, show premelting phenomena. Premelting phenomena in the small sized clusters is based on the fact that the surface atoms outside the core are more weakly bound than the core atoms, therefore, the amplitudes of these atoms are significantly larger than those in closed-shell clusters. This gives rise to enhanced harmonicities and provides fluidity in the system at lower temperature. In the large sizes, the clusters, no matter they have only closed shells as our cluster have, are expected to show premelting phenomena because of the surface reconstruction. As the cluster size increases, the surface atoms to core atoms ratio decreases and this gives the fact that the role of the surface atoms to the phase transition becomes less important. The size effects in phase transition are discussed by comparing our results with previously studied data.

We have also performed simulation on the fragmentation behavior of the cluster. The first atom is ejected by the cluster at $T = 2750$ K, then, second and third are at 3100 K and 3550 K respectively. By starting at 3850 K with the increasing

temperature, the larger atoms are being increasingly ejected for each 50 K temperature interval until the largest atoms, 37 atoms are ejected at 4850 K. The 429 atoms in the cluster is reduced to 155 at the temperature 5100 K. The criterion, Eq. (10), has been proposed that predicts the temperature at which the first atom evaporates in the nanoparticle.

References

1. Ş. Erkoç, in *Ann. Rev. Comput. Phys.* Vol. IX, ed. D. Stauffer (World Scientific Publ., 2001).
2. Ş. Erkoç, B. Güneş, and P. Güneş, *Int. J. Mod. Phys. C.* **11**, 1013 (2000).
3. Ş. Erkoç, *Phys. Stat. Sol. (b)* **152**, 447 (1989).
4. Ş. Erkoç, *Phys. Stat. Sol. (b)* **161**, 211 (1990).
5. V. Bonacic-Koutecky, P. Fantucci, and J. Koutecky, *Chem. Rev.* **91**, 1035 (1991).
6. I. M. L. Billas, J. A. Becker, A. Chatelain, and W. A. de Heer, *Science* **265**, 1682 (1994).
7. S. E. Aspel, J. W. Emmert, J. Deng, and L. A. Bloomfield, *Phys. Rev. Lett.* **76**, 1441 (1996).
8. A. Ghazali and J. C. S. Levy, *Phys. Lett. A* **228**, 291 (1997).
9. Y. E. Lozovik and E. A. Rakoch, *Phys. Lett. A* **235**, 55 (1997).
10. M. Schimidt, R. Kusche, W. Kronmüller, B. V. Issendorff, and H. Haberland, *Phys. Rev. Lett.* **79**, 99 (1997).
11. N. X. Sun, H. Lu, and Y. C. Zhou, *Phil. Mag. Lett.* **76**, 105 (1997).
12. F. Calvo and P. Labastie, *J. Phys. Chem. B* **102**, 2051 (1998).
13. C. L. Cleveland, W. D. Luedtke, and U. Landman, *Phys. Rev. Lett.* **81**, 2036 (1998).
14. Z. H. Jin and K. Lu, *Phil. Mag. Lett.* **78**, 29 (1998).
15. Y. E. Lozovik and E. A. Rakoch, *Phys. Lett. A* **240**, 311 (1998).
16. U. A. Salian, *J. Chem. Phys.* **108**, 6342 (1998).
17. A. Aguado, J. M. Lopez, and J. A. Alonso, *J. Chem. Phys.* **111**, 6026 (1999).
18. C. Chakravarty, *Phys. Rev. B* **59**, 3590 (1999).
19. M. H. Güven and M. Eryürek, *Phys. Stat. Sol.* (*b*) **213**, 283 (1999).
20. Z. H. Jin, H. W. Sheng, and K. Lu, *Phys. Rev. B* **60**, 141 (1999).
21. T. X. Li, Y. L. Ji, S. W. Yu, and G. H. Wang, *Sol. State Comm.* **116**, 547 (2000).
22. M. R. Ghayal and E. Curotto, *J. Chem. Phys.* **113**, 4298 (2000).
23. M. M. G. Alemany, C. Rey, and L. J. Gallego, *J. Chem. Phys.* **109**, 3568 (1998).
24. F. A. Lindemann, *Z. Phys.* **11**, 609 (1910).
25. J. F. Lutsco, D. Wolf, S. R. Philpot, and S. Yip, *Phys. Rev. B* **40**, 2841 (1989).
26. H. Hakkinen and M. Manninen, *Phys. Rev. Lett.* **55**, 1725 (1992).
27. S. N. Nayak, S. N. Khanna, B. K. Rao, and P. Jena, *J. Phys.: Condens. Matter* **10**, 10853 (1998).
28. X. Chen, J. Zhao, Q. Sun, F. Liu, G. Wang, and X. C. Shen, *Phys. Stat. Sol. (b)* **193**, 355 (1996).
29. A. Nordsieck, *Math. Comput.* **16**, 22 (1962).
30. C. W. Gear, *Numerical Initial Value Problems in Ordinary Differential Equations* (Prentice-Hall, 1971).
31. D. J. Evans and G. P. Morriss, *Comput. Phys. Rep.* **1**, 299 (1984).
32. J. Jellinek and I. L. Garzon, *Z. Phys. D* **20**, 239 (1991).
33. G. P. Johari, *Phil. Mag.* **77**, 1367 (1998).
34. J. Garcia-Rodeja, C. Rey, and L. J. Gallego, *Phys. Rev. B* **49**, 8495 (1994).
35. F. Calvo and F. Spiegelmann, *Phys. Rev. Lett.* **82**, 2270 (1999).

36. F. Calvo and F. Spiegelmann, *J. Chem. Phys.* **112**, 2888 (2000).
37. A. M. Mazzone, *Phil. Mag. Lett.* **78**, 145 (1998).
38. A. M. Mazzone, *Phil. Mag. B* **80**, 95 (2000).
39. P. T. Dinda, G. Vlastou-Tsinganos, N. Flytzanis, and A. D. Mistriotis, *Phys. Rev. B* **51**, 13697 (1995).
40. L. J. Lewis, P. Jensen, and J. L. Barrat, *Phys. Rev. B* **56**, 2248 (1997).
41. J. R. Christman, *Fundamentals of Solid State Physics* (John Wiley and Sons, 1998).
42. S. Valkealahti and M. Manninen, *Z. Phys. D* **26**, 255 (1993).
43. C. Kittle, *Introduction to Solid State Physics*, 7th edition (John Wiley and Sons, Inc., 1996).
44. A. Rytkönen, S. Valkealahti, and M. Manninen, *J. Chem. Phys.* **106**, 1888 (1996).
45. A. Rytkönen, S. Valkealahti, and M. Manninen, *J. Chem. Phys.* **108**, 5826 (1998).
46. T. Castro, R. Reifenberger, E. Choi, and R. P. Andres, *Phys. Rev. B* **42**, 8548 (1990).
47. E. Curotto, D. L. Freeman, B. Chen, and J. D. Doll, *Chem. Phys. Lett.* **295**, 366 (1998).
48. A. M. Mazzone, *Comput. Mater. Sci.* **18**, 185 (2000).
49. M. E. Garcia, D. Reichardt, and K. H. Bennemann, *J. Chem. Phys.* **109**, 1101 (1998).
50. A. Rytkönen and M. Manninen, *J. Chem. Phys.* **113**, 4647 (2000).
51. I. V. Hertel, C. P. Schulz, A. Goerke, H. Palm, and G. Leipelt, *J. Chem. Phys.* **107**, 3528 (1997).
52. *CRC Handbook of Chemistry and Physics* (CRC Press, 1974).
53. I. L. Garzon, I. G. Kaplan, R. Santamaria, and O. Novaro, *J. Chem. Phys.* **109**, 2176 (1998).